Perching and Resting – A Paradigm for UAV Maneuvering with Modularized Landing Gears

Kaiyu Hang[1*†], Ximin Lyu[2†], Haoran Song[2†], Johannes A. Stork[3,4†], Aaron M. Dollar[1], Danica Kragic[3], Fu Zhang[5]

[1]Department of Mechanical Engineering and Material Science, Yale University
[2]Hong Kong University of Science and Technology
[3]RPL, KTH Royal Institute of Technology
[4]Centre for Applied Autonomous Sensor Systems (AASS), Örebro University
[5]The University of Hong Kong
† These authors contributed equally in this work

*Kaiyu Hang; E-mail: kaiyu.hang@yale.edu.

Perching helps small Unmanned Aerial Vehicles (UAVs) extend their time of operation by saving battery power. However, most strategies for UAV perching require complex maneuvering and rely on specific structures, such as rough walls for attaching or tree branches for grasping. Importantly, many strategies to perching neglect the UAV's mission such that saving battery power interrupts the mission. We suggest enabling UAVs with a new capability of making and stabilizing contacts with the environment which will allow the UAV to consume less energy while retaining its altitude, in addition to the perching capability which has been proposed before. This new capability is termed as *Resting*. For this, we propose a modularized and actuated landing gear framework that allows stabilizing the UAV on a wide range of different structures

by perching and resting. Modularization allows our framework to adapt to specific structures for resting through rapid prototyping with additive manufacturing. Actuation allows switching between different modes of perching and resting during flight and additionally enables perching by grasping. Our results show that this framework can be used to perform UAV perching and resting on a set of common structures, such as street lights and edges or corners of buildings. We show that the design is effective in reducing power consumption, promotes increased pose stability, and preserves large vision ranges while perching or resting at heights. In addition, we discuss the potential applications facilitated by our design, as well as the potential issues to be addressed for deployment in practice.

1 Introduction

With recent advances in light-weight, low-power sensor technology and onboard computation, Unmanned Aerial Vehicles (UAVs) are now engaging in missions with an unprecedented degree of autonomy (*1–3*). Onboard sensors such as cameras, ultrasonic sensors, and accelerometers provide not only advanced perception capabilities that allow increasingly complex missions, but also enable more powerful control methods (*4–8*). Even commercial off-the-shelf (COTS) UAVs can reliably fulfill missions such as arial videography, autonomous surveillance, object delivery, construction site inspection, etc. (*9–13*) and are deployed in crisis response to provide on-site measurements (*2, 14–16*) or setup ad-hoc data networks (*17*).

Autonomous UAVs are often deployed to conduct long-duration missions which require watching over an area on the ground from heights for an extended period of time, such as in an autonomous surveillance task (*12, 18*). For this reason, energy consumption is one of the primal concerns in the operation of light-weight UAVs as mission duration is limited by battery

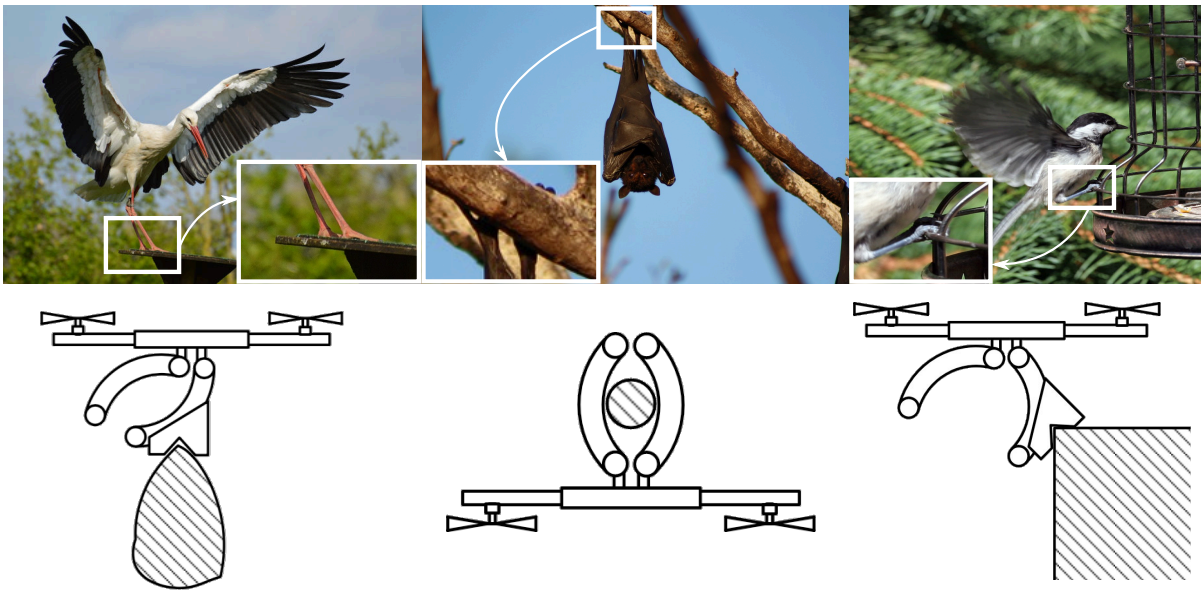

Figure 1: **Example perching and resting actions in nature:** Flying animals such as birds or bats often make use of structures in the environment to save energy. In choosing, they select locations that can be approached and evacuated by simply maneuvering in the air, while still allowing them to execute a mission – such as observing the environment or looking for prey.

power. Since UAVs require constant motor action to create lift in order to stay in the air, more energy efficient control and aircraft design are therefore of high interest to reduce the energy consumption during flight (*19–24*). However, the most effective way of saving energy is to directly reduce the required lift during execution of the mission.

1.1 Exploiting Contacts To Save Energy

In this work, we try to learn from nature and take inspiration from the behavior and anatomy of birds and bats. However, we propose a design that is simpler and more optimized for the specific task of saving energy than what we observe in nature. Figure 1, displays several ways in which animals with powered flight have adapted to temporarily exploit contacts with structures in their habitat for saving energy. For example, birds can be observed placing their feet on some support while still flapping their wings and bats are known to hang upside down while grasping some

suitable surface. In all of these cases, some suitably shaped part of the animal's foot interacts with a structure in the environment and facilitates that they have to generate less lift or that power flight can be completely suspended.

Our goal is to use the same concept, which is commonly referred to as *perching*, for UAVs. Perching requires attaching and detaching from a structure in the surroundings on command. However, it relies on the availability of certain structures in the surroundings, such as tree branches. It is therefore limited to a small set of mission environments and more importantly, when the perching location does not provide a good view range, it will result in mission interruptions. For addressing the problem of allowing UAVs to reduce their power consumption in a mission, we propose to enable UAVs with the capability of making and stabilizing contacts with the environment to obtain force support. With this capability, UAVs require less lift generated by the motors and can save energy. Moreover, it enables UAVs to be able to exploit a much larger range of structures in the environment to conduct missions without interruptions. We term this kind of actions as *Resting* (Figure 1, left and right). Perching or resting on elevated locations allows continuation of a large range of UAV missions with reduced, or even suspended, motor action and therefore extends the UAVs operation time and allows for long-duration missions, such as in the most common perch-and-stare missions (*25*). Additionally, perching and resting remove degrees of freedom from the UAV's motion and can therefore reduce the required attention from operators and can improve safety.

The need for perching capabilities in UAVs leads to research in a wide range of different forms of landing gears (*26–44*), control for the required flight regimes, and the generation and optimization of approach trajectories (*30–32, 37, 38, 45–47*). Surface contacts can be established and maintained with dry adhesive technology such as electrostatic surfaces (*41–43*) or fibers (*44*). A collection of small needles can be employed for perching on rough surfaces (*26–31*) or be combined to bio-inspired claw-like grippers (*33*). Also, multiple tensile

anchors can be launched to fixed structures (*48*) to mechanically stabilize the UAV for high accuracy operation in 3D workspace. Other UAV-mounted grippers take design inspiration from the feet of songbirds for perching on branch-shaped structures (*37–40*). Furthermore, grippers can be used to attach to flat surfaces (*32, 46*) and in some cases also serve as landing skids when opened (*36*). In general, passive and compliant grippers can wrap around structures (*34, 39–41*), while actuated grippers can actively grasp a structure to attach the UAV (*33, 36*).

1.2 The Challenges

However, approaches based on dry adhesive (*41–44*) or small needles (*26–31*) have only been demonstrated for extremely light-weight UAVs and require specific UAV design to allow proper positioning of the landing gear for perching. Therefore, these approaches are difficult to adapt to COTS UAVs or UAVs that carry a heavy sensor payload such as a high-resolution camera. Also, while avian-inspired grippers can be mounted on COTS UAVs, most gripper-based approaches are limited to perching cylindrical structures of a certain diameter (*36*).

As another very important component for perching, control has to address a challenging problem since the UAV needs to be positioned close to a structure. Different from flight in open space, this is often done with flight regimes involving high angle of attack (*47*), post stall (*45*), or aggressive (*32, 46*) maneuvering in order to bring the landing gear to the required attitude and location while the UAV reaches a flight condition that allows safe contacting on the structure. In bio-inspired approaches this can be done directly from feedback without optimizing the flight trajectory explicitly before the flight (*37, 38*). For maneuvering while in contact with a pivot point on a structure, dynamic modeling of the different flight phases is necessary (*49*).

However, the flight regimes for attaching and detaching are in many cases complex and are not covered by control for COTS UAVs. For instance, approaches that perch on walls and have the landing gear mounted below the UAV have to fly towards the wall and turn the bottom side

forward for attaching (*26–32, 46*). Failure to attach will result in a critical flight condition close to an obstacle. These risks are shared with approaches that employ high angle of attack (*47*) and post stall (*45*) maneuvers for perching. Perching on walls can also require a mechanism-supported takeoff strategy that puts the UAV in a critical flight condition after detachment (*26*).

Most importantly, many approaches are not focussed on continuing the UAV's mission and can therefore lead to mission interruption when perching. For instance, in approaches that rely on surfaces for perching, the UAV has to comply to the surface's orientation (*26–32, 46*) which might obstruct sensors or communication devices. As a result, it is still challenging to enable perching capabilities in COTS UAVs under a wide range of circumstances without disrupting the mission or requiring risky and complex maneuvering that involves critical flight conditions.

1.3 A New Paradigm for Perching and Resting

As mentioned above, we observe in nature that (perching) birds and bats have adapted to their habitats by developing prehensility and claws in their feet, which allows them to use a large variety of structures for support when perching (see Figure 1). Instead of directly imitating for instance the feed of perching birds (passerine birds), we propose a simplified and specialized solution for COTS UAVs. Based on four design principles, we design a modularized and actuated *landing gear framework* for rotary-wing UAVs consisting of an actuated *gripper module* and a set of *contact modules* that are mounted on the gripper's fingers. The gripper module is mounted on the bottom side of the UAV and, for its weight and size, is compliant with a large range of COTS UAVs. Unlike previous approaches with grippers (*37–40*) our approach is not limited to cylindrical structures only and does not require complex attachment maneuvers such as a sideways approach (*32, 46*).

If a horizontal surface is available, the gripper module is opened and the stiff fingers are used as landing skids, similar to a bird landing on a flat rooftop. If a cylindrical structure

is available, the UAV approaches it from above such that the gripper module can grasp the structure after which all motors can be suspended. This is directly inspired by how birds land on branches of trees to which they then hold on. For other types of structures such as edges or corners of a buildings, struts, bars, or street signs, we rely on modularization, allowing us to flexibly design and fabricate contact modules that match the specific structure. Through gripper actuation and position control, a suitable contact module is then brought to rest on the structure and all or a part of the UAV's weight is supported by the structure, reducing the required lift. This modularization substantially increases the range of possible structures that can be exploited for perching and resting as compared to avian-inspired grippers. While not inspired by nature and much more simple than the foot of a bird, the stiff fingers and contact modules are easier to manufacture and more robust and durable than avian-inspired grippers with several joints per finger.

Takeoff and landing are critical phases in a flight and it is known that for example pigeons show complex pattern of wing strokes for acceleration and deceleration during maneuvers (*50*). However, while we take inspiration from how birds and bats rest, we do not imitate their maneuvering for landing or taking off since the UAV as a rotary wing aircraft has significantly different flight characteristics from birds and bats with flapping wings. In contrast to previous approaches (*32, 37, 38, 45–47*), we develop an approach that relies on position control and reference poses only, without requiring complex control strategies. For perception, we present a proof-of-concept method that identifies suitable structures for perching and resting from point cloud data of the environment.

Overall, we in this work investigate 4 fundamental questions of UAV maneuvering in terms of the exploitation of external contacts: 1) How to design landing gears to facilitate UAVs to exploit contacts for perching and resting; 2) How is the energy consumption and pose stability affected by perching and resting; 3) How is the mission-relevant view ranges of UAVs affected

by different perching and resting actions; and 4) What are the use cases and limitations of the proposed paradigm.

In experiments, we mount our landing gear framework on an COTS UAV and demonstrate the efficacy of our design in enabling the desired perching and resting capabilities in a controlled laboratory environment. The experiments include perching and resting on different structures and their perception. During the experiments, the UAV is globally localized with an external measurement system. In this setting, we evaluate power consumption and pose stability during perching and resting for empirical comparison to hovering. Furthermore, we qualitatively study the view ranges of different perching and resting actions on locations at heights and discuss other potential usage in terms of the features enabled by perching and resting. Our experiment results show that the proposed paradigm not only reduces energy consumption, but also enables UAVs to exploit external contacts with a variety of structures to facilitate mission execution, which, to the best of our knowledge, has not been extensively studied.

2 Results

Our modularized and actuated landing gear framework is designed to be flexible and accommodate to a wide range of applications. In order to demonstrate and evaluate the principles and efficacy of our design, we present a proof-of-concept study in which we design and fabricate a landing gear for a DJI F450 quadrotor platform and test the resulting perching and resting capabilities in a number of scenarios with different structures. Since most recent UAV applications involve load-carrying for videography or surveillance, we evaluate the perching and resting states in terms of (a) power consumption, (b) pose stability, and (c) view ranges.

We fabricate the gripper module's base and fingers using carbon fiber to keep the landing gear rigid and light-weight. The contact modules are 3D printed using the soft TangoBlackPlus™ material to facilitate contact compliance and stability for a wide range of environments. The

weight of each part of our landing gear framework is listed in Table S1. In the experiments, the environment is perceived using an externally placed Kinect One™ sensor which provides point clouds in which we detect structures that allow perching and resting. Once contact locations in the environment are identified, as shown by colored points in Figure 2 and Figure 4, the UAV is autonomously navigated based on the localization provided by a VICON system. An example lab setup for our experiments is shown in Figure 2.

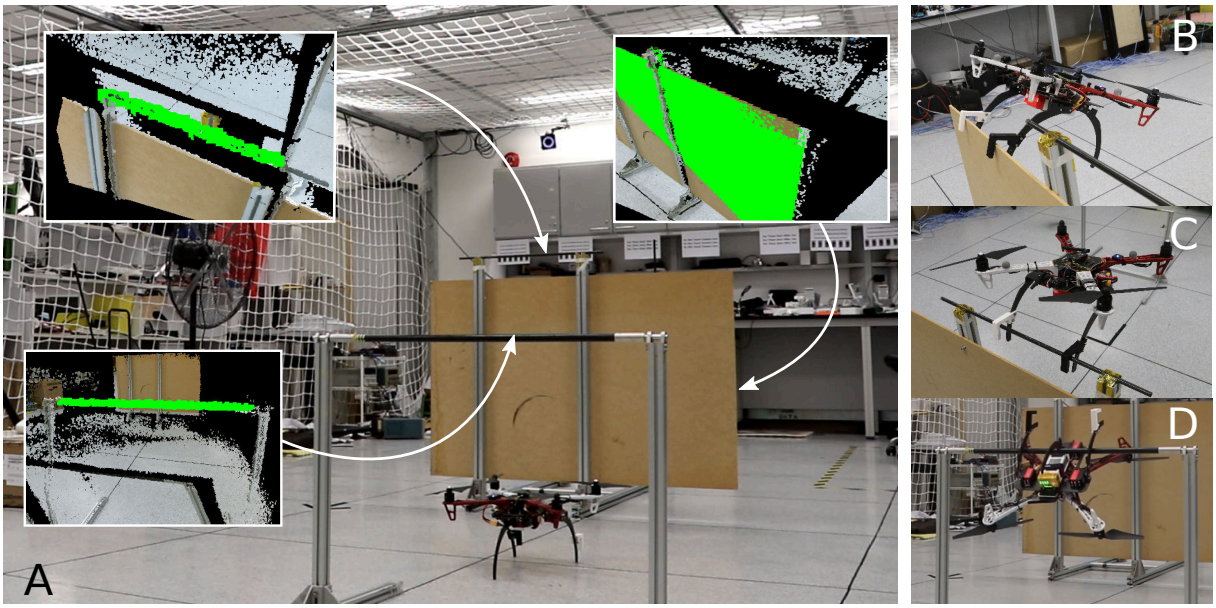

Figure 2: **Example actions with vision-based perching and resting location detection:** (**A**) Lab environment and detected perching and resting locations. (**B**)Perching by hooking on a thin board (P_H). (**C**)Resting by hooking on a stick (R_H). (**D**)Perching by grasping around a stick (P_G).

2.1 Landing Gear Design

In this section, we first describe the design principles of the proposed modularized landing gear framework. Based on the principles, we demonstrate our example design and evaluate its performance.

2.1.1 Principles of Landing Gear Design for Perching and Resting with COTS UAVs

In order to enable perching and resting under various circumstances while keeping the design versatile, we propose to design landing gears obeying four principles:

1. The landing gear should be usable for landing on flat surfaces, mirroring the capabilities of most standard landing gears for COTS UAVs. This allows the UAVs to land and take off as usual COTS UAVs.

2. The landing gear should allow the UAVs to grasp or hook around structures of different scales. This allows the UAVs to turn all rotors off when perched.

3. The landing gear should allow the UAVs to rest on different structures to provide lift support in the vertical direction. This allows the UAV to slow down or completely stop some of the rotors when resting by establishing stable contacts with the environment.

4. The landing gear should be mountable on a COTS UAV and be minimalistic in hardware, actuators, and control. This allows the user to design and replace parts of the landing gear without the need of reprogramming when working in different scenarios.

Following the principles, we demonstrate an example design consisting of an actuated gripper module that features the principles 1, 2 and 4, and a set of contact modules that features principles 3 and 4.

2.2 Actuated Gripper Module

The actuated gripper module consists of servomotors, a set of fingers, and a base platform which is attached to the bottom of the UAV. Our landing gear design for the DJI F450 UAV with 3 fingers is shown in Figure 3. On the base platform, the 3 servomotors are installed to actuate the open and close motions of the fingers. In order to ensure sufficient grasping

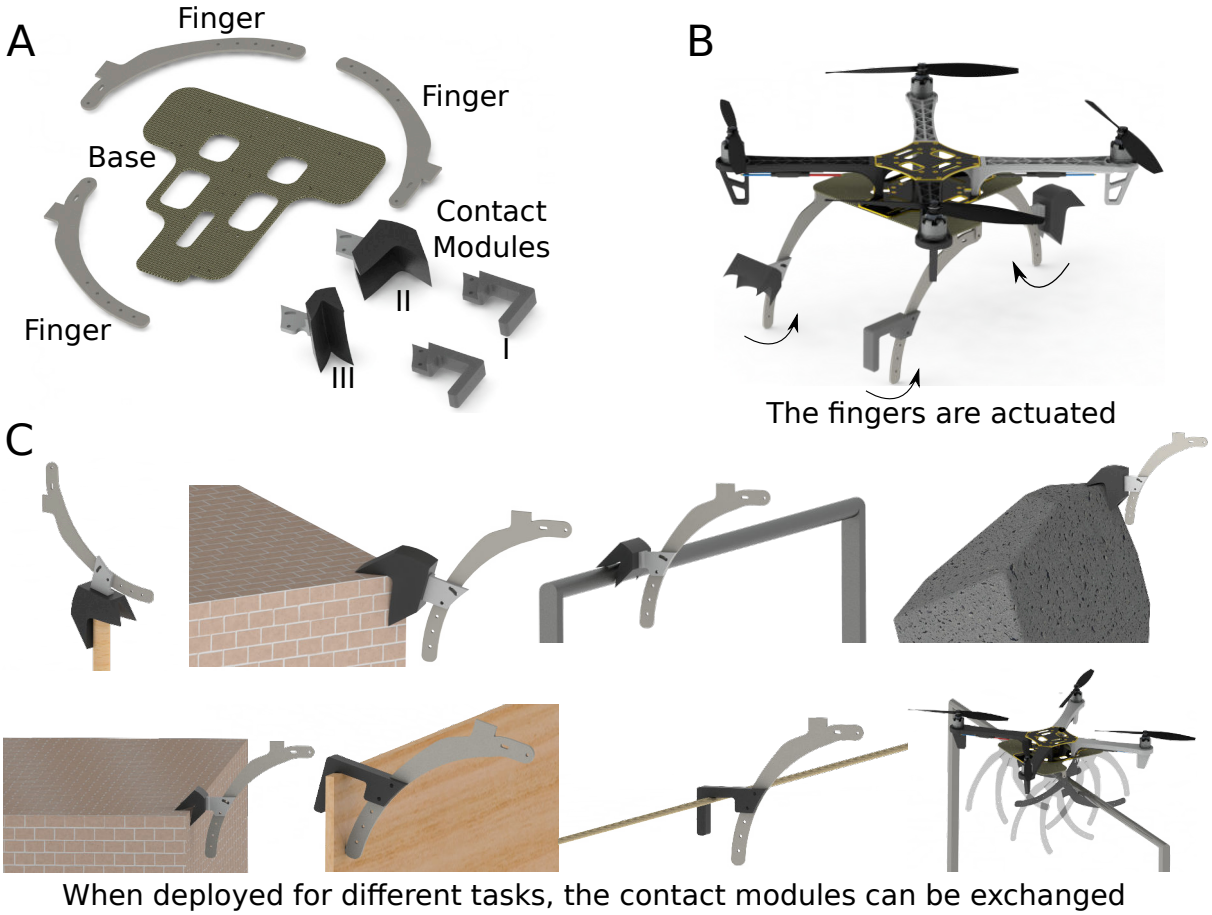

Figure 3: **An example landing gear design for DJI F450:** (**A**)An example of the modularized landing gear design consists of a base, 3 fingers and 3 different contact modules. (**B**)An example of the installation of the designed modules on a DJI F450 platform. (**C**)Example perching and resting actions using different contact modules or actuated gripper module.

forces, the 3 servomotors are adopted to actuate the fingers separately. However, the motors are controlled jointly for open and close actions with only 1 DoF. In practice, all fingers can be actuated by a single motor as long as the provided torque is sufficient for the grasping actions. When the gripper is opened, the fingers enable normal landing and take-off from the ground as the fingertips are in level position under the UAV.

As seen in Figure 3, the size of the landing gear is approximately identical to the UAV's dimensions. This enables the UAV to grasp structures of up to 0.2m in radius. However, deciding on the dimensions of the gripper module is a trade-off between the size of potential perching structures, the gripper weight, undesired aerodynamical side-effects, and collision-free maneuvering. A larger gripper can accommodate larger structures but can lead to loose contact for small structures. Our design makes it easy to replace the fingers and it is recommended to design the fingers in appropriate sizes to achieve the tasks while avoiding undesired side-effects. Additionally, the design of the gripper fingers should guarantee that it makes a closed loop when in close position, which ensures the perching ability on all structures within the scale of the landing gear.

2.3 Contact Modules

According to the design principles, we equip the UAV with different contact modules that are easy to use, design, and fabricate. Inspired by the claws of birds, we design the contact modules such that they are able to stabilize the UAV with different structures in the environment by contacting their modeled side, which acts similar to claws to hold onto small or thin structures. As shown in Figure 3, contact modules are installed at the distal-ends of the fingers making them accessible to structures below the UAV. For resting, the gripper module is actuated to bring the contact module to the desired pose. This can be an open pose for contacts on one side of the UAV as seen in Figure 4 or a closed pose for contacts below the center of the UAV as

seen in Figure 4. The contact modules themselves are not actuated for actively stabilizing the contacts. Instead, their shapes are adapted to achieve stable contacts against certain structures. Based on the minimalistic and modular design principles, the contact modules are exchangeable to provide more contact possibilities with a large variety of geometries.

In this work, we exemplify a few contact module designs that are based on the concept of *Contact Primitives* and fingertip surface optimization (*51*). The algorithm synthesizes contact modules based on a set of example structures. As long as the provided examples sufficiently represent potential contact structures, the synthesized contact modules will be able to stabilize the contacts. Figure 3 shows 2 contact modules (II and III) that were synthesized by the algorithm. Additionally, similar to claws that birds use to grasp and perch, we designed another L-shaped contact module which, together with the finger, creates a U-shaped claw. As shown in Figure 3, this design allows for perching on thin structures on which a UAV can hook itself using gravity.

2.4 Saving Power by Reducing Motor Action

In this work, we exemplify 5 perching or resting actions using the experimental UAV for demonstration and evaluation. As seen in Figure 2 and Figure 4, the actions are perching by hooking (P_H), perching by grasping (P_G), resting by hooking (R_H), resting on an edge (R_E) and standresting on a stick (R_S).

Power consumption is one of the major concerns for many UAV applications and the main goal of our design is to save battery power by reducing motor action for generating lift. For this reason, we analyze energy consumption in examples of perching and resting, and compare them to the energy consumption while hovering in the air or above the floor.

If the UAV is perching by grasping around a structure (P_G) or hooking on a thin structure (P_H), as seen in Figure 2, its weight is fully supported by the structure and all the rotors can be

Figure 4: **Example resting actions with vision-based perching and resting location detection:** (**A**)Resting on a box's edge (R_E). (**B**)Stand-resting on a stick (R_S).

turned off. Therefore, the energy consumption is 0.

When using a contact module below the center of the UAV for resting, as seen by the action R_S in Figure 4, all the rotors still need to be used for maintaining the balance. However, the rotors can be dramatically slowed down since the load is mainly supported by the structure. When using contact modules for resting on a structure below the side of the UAV, as shown by the action R_E in Figure 4 and R_H in Figure 2, the UAV has to only maintain 2 degrees of freedom, which are the rotation about the contact line and sliding along the contact line. In those cases, two rotors can be completely turned off.

Empirical results are reported in Figure 5. The power consumption data is recorded from the point when the UAV has stabilized itself and ends when the UAV takes off again. As can be seen from the figure, the stand-resting action R_S consumed the least energy since almost all the load was supported by the contact. When resting on the box edge R_E or on the stick R_H, power consumption was higher, which was up to about half of the energy consumption of the hovering action. It is worthwhile noting that these two resting actions consumed a bit more power than

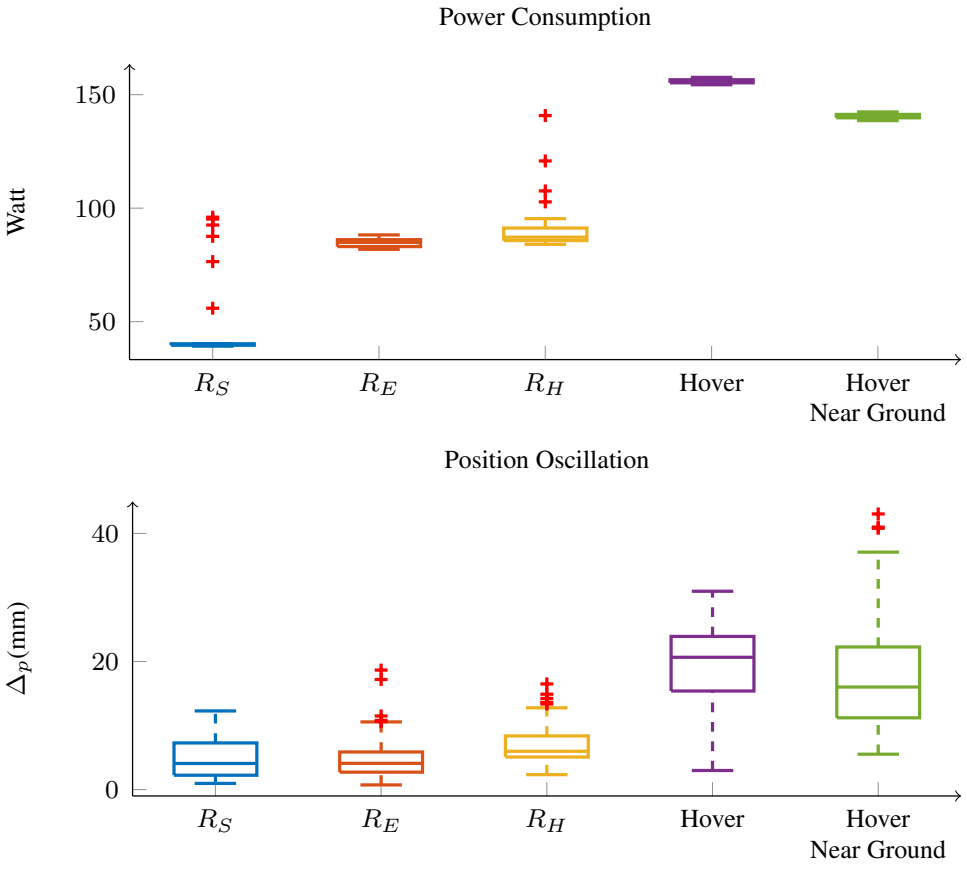

Figure 5: **Power consumption and stability evaluation results.** For measuring the power consumption, we take the measurement directly from the motors without considering the power consumed by other electronics. On each box plot, the central mark indicates the median, and the bottom and top edges of the box indicate the 25th and 75th percentiles, respectively. The whiskers extend to the most extreme data points not considered outliers, and the outliers are plotted individually using the '+' symbol.

half of the hovering. This is because the UAV needed to counteract the ground effect when it was very close to other objects. Lastly, we can see that when hovering near ground, due to the ground effect, the UAV consumed a little less energy than hovering in the air. In comparison to hovering in the air, R_S, R_E and R_H saved 69%, 46%, 41% power consumption respectively.

2.5 Evaluating Stability and View Range

For many applications such as videography, surveillance, or object delivery at heights, stable positioning of the UAV over a period of time is necessary. For this reason, we evaluate position oscillation Δ_p with respect to a reference location $\overline{p} = (\overline{x}, \overline{y}, \overline{z})$ for different perching and resting scenarios. For this, we define $\Delta_p = \frac{1}{T}\sum_{i=1}^{T}\sqrt{(x_i - \overline{x})^2 + (y_i - \overline{y})^2 + (z_i - \overline{z})^2}$, where (x_i, y_i, z_i) is the location sampled at time i, $1 \leq i \leq T$. Since the UAV's position is passively determined when all rotors are turned off, we only evaluate the position oscillation for resting actions when the stability is actively determined by the control of rotors.

As reported in Figure 5, hovering results in oscillation are within a small range of about 2cm. However, resting is even more stable and maintains the desired pose within approximately 5mm. By checking the standard deviations, we can see that the standard deviations of resting were less than half of that of the hovering actions. These results show that resting can provide more stability while at the same time can reduce power consumption.

Especially in perch-and-stare missions, the UAV's view range is a crucial concern when it is tasked to stare or watch over a certain area. However, landing on a flat elevated position such as a rooftop can significantly reduce the UAV's view range. Figure 6 shows how the rooftop occludes most of the view ranges below when a UAV lands on it. Compared to that, perching or resting as offered by the modularized landing gear framework, can improve the view range. In most cases, the UAV can fully observe the area below it without any occlusions. An exception case is seen when a UAV rests on the edge of a building, which occludes about half of the view

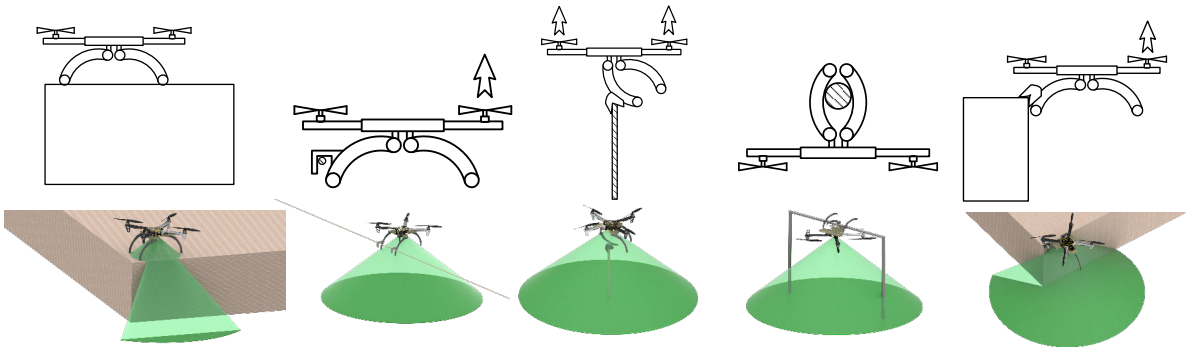

Figure 6: **Example view ranges of different perching and resting actions:** The upper row shows various perching and resting actions with arrows indicating which rotors are still working for generating lift. The lower row shows the corresponding view ranges rendered by green cones.

below. Nonetheless, it is still much better than a normal landing on the roof.

It is worthwhile noting that, upon using different perching or resting actions, the on-board camera can be configured accordingly to optimize the view. For example, when perching on a stick by using the actuated fingers to grasp, the UAV will finally be stabilized after it turns over around the stick and stops all its rotors. As such, differently from most UAVs which have the camera installed below the main frame, the camera, or an extra camera, should be installed on top of the UAV to achieve the view range when the UAV turns over and faces downwards.

3 Discussion

In this section, we first give a brief summary of what has been proposed and evaluated. Thereafter, we discuss the limitations and implementation concerns of our design, the concerns in pose stability and energy consumption in relation to our paradigm, as well as the use cases of the proposed design framework.

In this work, we focused on the problem of enabling perching and resting for rotary-wing UAVs. First, we proposed to enable UAVs with the capability of making and stabilizing contacts with the environment, so as to obtain force supports from the contacts to be able to consume

less battery energy while retaining the heights. For this, we developed a design framework of modularized and actuated landing gears consists of an actuated gripper module and customized contact modules. The goal is to permit lower power consumption, better stability, and larger view ranges when the task is to be executed at fixed locations at heights. Following the 4 design principles, we designed an example landing gear for a DJI F450 quadrotor. The example design is composed of a base platform, 3 actuated fingers which were fabricated using carbon fibers, and 3 customized contact modules which were 3D printed using soft materials. The design resembles the basic functionalities of normal landing gears allowing for landing and take-off actions, and is light-weight for the UAV to carry on-board while not introducing much more extra power consumption.

We validated the example design by demonstrating perching and resting under lab conditions, such as perching by grasping and hooking, resting on an edge or stick, and stand-resting on a stick. The stability and power consumption of demonstrated actions have been evaluated, and the results indicate that the featured actions can significantly reduce the power consumption, while providing better stability comparing to normal actions. Additionally, we have qualitatively shown that the featured actions provide much larger view ranges when working at heights, which can hardly be achieved by normal landing actions.

3.1 Limitations and Implementation in Practice

In this work, our experimental quadrotor was not equipped with on-board vision capability. The perching and resting locations were detected based on the point cloud obtained by an external Kinect One sensor beforehand, and the UAV was navigated by a VICON system in the lab environment. In practice, when maneuvering a UAV in outdoor environments, the on-board visual perception is important to help the human operator to navigate, or to enable the UAV itself to be more autonomous. When a UAV is tasked to autonomously execute the perching or resting

actions, an on-board visual sensor is required to enable the UAV to understand the environment, as well as to detect the locations where desired actions can be applied on. As will be described shortly, given that the modularized landing gears is flexibly customized for accommodating a certain range of task requirements, the vision algorithms can be designed using template-based approaches that match geometrical features between the environment and the designs. Nevertheless, the vision based detection approach is intrinsically limited that it is not easy to acquire physical properties of the environment, such as the rigidity of the detected locations which can affect the action stability. For addressing this problem, learning based algorithms can be adopted to predict the physical properties. More reliably, active perception algorithms can be developed to conduct physical estimation by enabling the UAV to actively interact with the environment, e.g., a UAV can use its contact modules to touch and press certain locations to acquire knowledge, which can potentially be obtained by additional sensors installed on the contact modules.

Additionally, in our experiments, our control strategy is to always navigate the UAV to a waypoint above the perching or resting locations, and then execute the action from top-down. However, in many tasks in reality, one can imagine a UAV working in confined environments, in which the perching or resting actions cannot be executed without a trajectory planning algorithm. As discussed in (*38, 52*), we can enable the UAV with trajectory planning to perch or rest in more difficult scenarios by bringing the UAV to the desired location without the top-down motion constraint. For instance, a UAV can perch on a tree branch by approaching it from the side and grasping it with the fingers when the region above that tree branch is occluded.

3.2 Pose Stability and Energy Consumption

As the main goals of the proposed paradigm, pose stability and energy consumption have been evaluated using an example design in a lab environment. The experimental results have shown

that both perching and resting actions can significantly reduce the power consumption by exploiting force support from external contacts. In addition, using the same flight controller, we have seen that pose stability has been improved when external contacts are made. This can be explained by the fact that, when contacts are made between the contact modules and external structures, the degrees of freedom of the UAV's movement is reduced. As such, the potential external disturbance is reduced, and more importantly, the flight controller can focus on balancing only the remaining degrees of freedom, mitigating the trade-off of keeping pose stabilities between different moving dimensions.

Nonetheless, we can foresee a variety of factors that can affect these two performance concerns. When a UAV is tasked to work in outdoor environments, wind disturbance and other aerodynamic uncertainties can be a major factor that affects pose stability. In this case, the flight controller will have to regulate the actuation inputs more intensively to keep the stability at a similar level, resulting in increased energy consumption. Moreover, the rigidity or mobility of contact locations can be another concern that affects the pose stability. For example, when resting by making contacts at a thin tree branch, although the UAV can gain force support to reduce energy consumption, it is more difficult to keep stability due to the passive movement of the contacts, and will consume more motor energy in comparison to making contacts at rigid locations. In order to reduce the effect of physical uncertainties and improve the energy performance, although not included in this work, we plan to design a tilt-pan connector between the main body of the UAV and the modular landing gear. By mechanically decoupling the movement of the UAV's main body from the landing gear, or by actively compensating the disturbances at the connector, the pose stability can be further improved. Limited by the scope of this study. we leave this development to our future work.

3.3 Use Cases

A UAV with perching and resting capabilities can enable many applications that are not possible otherwise. Besides that perching and resting can provide lower power consumption, better stability and larger view ranges in many cases, which is very useful for perch-and-stare applications, the physical interaction with the environment enabled by such actions additionally empower many more applications. For example, in aerial grasping (*53–55*), the maximum load is limited by the power provided by the rotors. However, once a UAV is perched, it will be able to lift dramatically larger loads without requiring any power from the rotors.

When delivering objects to workers at heights, a UAV can perch or rest at some location near the worker for objects pickup; or it can carry a pair of pulley and rope to perch at a certain location, such that objects delivery can be achieved from both ends of the rope. While resting at the edge of a windowsill, a UAV will be able to deliver objects to someone inside, without the need of keeping the rotors at the window side still working, so as to reduce the risk for humans to interact with a UAV. Overall, the ability of making contacts by resting or fixing itself by perching at heights empower many applications that are load-lifting related and interaction demanded.

4 Materials and Methods

In addition to the design of the proposed modularized landing gears, we in this section briefly describe how to enable a UAV with such landing gears to execute the perching and resting actions in reality. Concretely, we will introduce how we implemented the vision algorithm to detect perching and resting locations, how the UAV is controlled, and how to automatically design contact modules based on example contacts.

4.1 Perching Locations Detection and Navigation

As the main focus, we in this work concentrate on the design of modularized landing gears and evaluated our example design installed on a DJI F450 platform. For the experiments, we did not install an on-board camera for the UAV to detect perching locations, nor other sensors to navigate it in the environment. Instead, we 3D scanned the lab environment beforehand and saved a point cloud of the environment. For perching location detection, we implemented a hybrid system based on the PCL library (*56*) to detect feasible perching and resting locations. Concretely, as shown in Figure 7, the system takes the environment point cloud as the input and first needs to decide whether a perching location or a resting location is desired. In practice, we always try to find perching locations first, and then will look for resting locations if the former is not available.

If a perching location is desired, in addition to the environment point cloud, the system will be provided with a set of shape primitives which are preferable for perching actions. In our examples, we showed perching by grasping on a stick and perching by hooking on a thin board. In order to detect such locations in a point cloud, we used the Random Sample Consensus (RANSAC) algorithm based on parameterized shape templates, and the results are shown in Figure 2. For detecting resting locations, given that those actions rely on the customized contact modules, the detection is also based on the shapes of contact modules. As depicted in Figure 7, the Fast Point Feature Histograms (FPFH) are extracted from both the environment point cloud and the contact modules. Thereafter, we try to register the contact modules to feasible locations in the environment and optimize the results using the Iterative Closest Point algorithm (ICP).

Once a perching or resting locations is found, it needs to be verified by 2 additional steps. Since the UAV always approaches those locations from top-down in an up-right pose, we check whether the surrounding area is collision free and whether the area allows for top-down approaching motions. As a negative example, for resting on an edge, the UAV can not stabilize

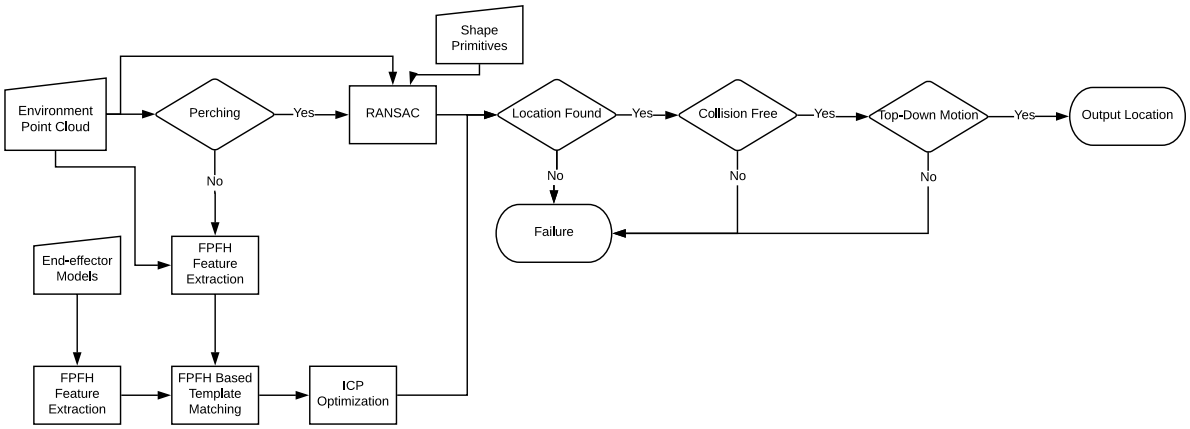

Figure 7: **Flowchart of the hybrid system for perching and resting locations detection.**

itself by making contacts on the side-edges of a box or a building, the edge has to be on top and approximately horizontal. Once a perching or resting locations is confirmed, the coordinates of it is transformed to the VICON system and the UAV will be navigated to apply the action.

4.2 Perching and Resting Control

To execute the actions for perching and resting, we apply a flight controller which mixes the the position control and attitude control of the UAV in a cascaded manner. The details of the controller design is provided in Appendix. S1. For perching actions, the UAV first navigates to the desired location, and once the grasping or hooking actions is applied, the UAV turns off all the rotors and stays in the perching mode. In case the UAV needs to turn over, we apply a proportional angular velocity controller to realize a smooth motion.

For resting actions, the UAV also needs to first navigate to the desired location. However, differently from the perching actions, the UAV will only turn off or slow down some of the rotors. In cases when one side of the UAV can totally rest on some structures, such as edge resting, the rotors at the corresponding side can be turned off, and the rest of the rotors should still work to support the weight. In another case when the UAV can not totally rest on any side,

such as the stand-resting, the UAV can slow down the rotors but still need some lift to keep the balance.

In both of the above cases, we aim at minimizing the power consumption to stabilize the UAV at the desired pose. This is achieved through the cascaded controller using a shifted reference point. Concretely, denoted by $\mathbf{p} \in \mathbb{R}^3$ the location of the UAV at the resting location. If we command the UAV to stay at $\mathbf{p}$, the rotors will still work at full speed to realize the precise pose control. In order to automatically slow down the rotors while keeping the UAV at the desired resting pose to stabilize contacts, we introduce a shifting factor $\Delta_r \in \mathbb{R}^3$ to shift the reference point towards the direction from which the UAV will obtain the resting support. Once the UAV has reached the resting location $\mathbf{p}$, the reference point for the controller will be shifted to $\mathbf{p} - \Delta_r$ and the rotors at the supported side will be stopped. Due to the physical contacts, the UAV in practice is not able to achieve the shifted reference. However, it slows down the rotors to try to approach it while keeping the pose upright. Additionally, as the UAV would try to approach the shifted reference point, it will actively exert force at the contacts, this effect can further improve the stability of resting actions.

4.3 Contact Module Design

The contact modules are used to passively stabilize the contacts between the landing gear and the resting locations. Therefore, we aim at generating contact modules with shapes that can maximally resemble the typical contact geometries that are available in the environment. In order to keep the design general enough to accommodate as many scenarios as possible, we adopt the fingertip design algorithm from (*51*).

Concretely, the contact module design is formulated as an optimization problem addressed in three steps. Firstly, given a working environment of the UAV, we provide the algorithm with a set of example shape primitives, which are representatives for describing typical shape ge-

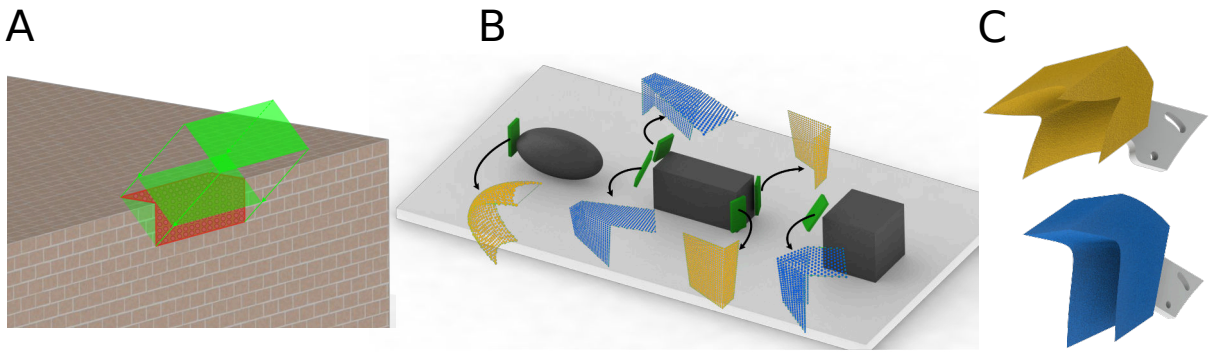

Figure 8: **Example contact area extraction for automatic contact module design.** (**A**) An extraction of a contact area (red) based on the specified contact pose and size. (**B**) The shape primitives (black) and the extracted contact areas (clustered in blue and yellow) used in the contact module design in this work. (**C**) The contact modules designed in terms of the clustered contact areas.

ometries in the working environment. Thereafter, as shown in Figure 8, by specifying a set of example contact poses, the algorithm extracts a set of contact areas that will be potentially used for resting contacts in the environment, and represents them as point clouds. Secondly, the algorithm automatically determines the number of clusters, and then clusters the extracted contact areas into different groups, in terms of the geometric similarities between them. Finally, modeled by a parameterized 3D surface for each contact module, the algorithm optimizes the module's surface shape by minimizing the differences between the surface and all the contact areas in the corresponding cluster. As such, the optimized contact module's surface will maximally resemble the geometric features of the potential contacts, and will improve the stability of contacts for the UAV to rest at the corresponding locations. For more detailed explanation of this algorithm, we refer the readers to (*51*).

In this procedure, the more example contact areas are provided to the algorithm, the more clusters of contact areas will be potentially produced, and so the number of designed contact modules. This enables the UAVs to rest at a variety of different locations, since the contact modules can be exchanged when working in different environments. Additionally, it is worthwhile

noting that, although the designs are maximally resembling the geometric features of contact areas, there are always differences between the designed contact module and the real contact locations in the environment. In order to minimize the effects given by this difference, we suggest to fabricate the contact modules using soft materials, so that some small differences at contacts can be compensated to improve the stability of contacts.

References

1. C. Goerzen, Z. Kong, and B. Mettler, "A survey of motion planning algorithms from the perspective of autonomous uav guidance," *Journal of Intelligent and Robotic Systems*, vol. 57, no. 1-4, p. 65, 2010.

2. T. Tomic, K. Schmid, P. Lutz, A. Domel, M. Kassecker, E. Mair, I. L. Grixa, F. Ruess, M. Suppa, and D. Burschka, "Toward a fully autonomous uav: Research platform for indoor and outdoor urban search and rescue," *IEEE Robotics and Automation Magazine*, vol. 19, no. 3, pp. 46–56, 2012.

3. S. Rathinam, P. Almeida, Z. Kim, S. Jackson, A. Tinka, W. Grossman, and R. Sengupta, "Autonomous searching and tracking of a river using an uav," in *American Control Conference*. IEEE, 2007, pp. 359–364.

4. A. Ryan, M. Zennaro, A. Howell, R. Sengupta, and J. K. Hedrick, "An overview of emerging results in cooperative uav control," in *IEEE Conference on Decision and Control*, vol. 1. IEEE, 2004, pp. 602–607.

5. J.-H. Kim, S. Sukkarieh, and S. Wishart, "Real-time navigation, guidance, and control of a uav using low-cost sensors," in *Field and Service Robotics*. Springer, 2003, pp. 299–309.

6. S. Lange, N. Sunderhauf, and P. Protzel, "A vision based onboard approach for landing and position control of an autonomous multirotor uav in gps-denied environments," in *IEEE International Conference on Advanced Robotics*. IEEE, 2009, pp. 1–6.

7. W. Pisano, D. Lawrence, and P. Gray, "Autonomous uav control using a 3-sensor autopilot," in *AIAA Infotech@ Aerospace Conference and Exhibit*, 2007, p. 2756.

8. S. Ross, N. Melik-Barkhudarov, K. S. Shankar, A. Wendel, D. Dey, J. A. Bagnell, and M. Hebert, "Learning monocular reactive uav control in cluttered natural environments," in *IEEE International Conference on Robotics and Automation (ICRA)*. IEEE, 2013, pp. 1765–1772.

9. G. Zhou, J. Yuan, I.-L. Yen, and F. Bastani, "Robust real-time uav based power line detection and tracking," in *IEEE International Conference on Image Processing*. IEEE, 2016, pp. 744–748.

10. I. Maza, K. Kondak, M. Bernard, and A. Ollero, "Multi-uav cooperation and control for load transportation and deployment," in *International Symposium on UAVs*. Springer, 2009, pp. 417–449.

11. P. E. Pounds, D. R. Bersak, and A. M. Dollar, "Stability of small-scale uav helicopters and quadrotors with added payload mass under pid control," *Autonomous Robots*, vol. 33, no. 1-2, pp. 129–142, 2012.

12. E. Semsch, M. Jakob, D. Pavlicek, and M. Pechoucek, "Autonomous uav surveillance in complex urban environments," in *IEEE/WIC/ACM International Joint Conference on Web Intelligence and Intelligent Agent Technology*. IEEE Computer Society, 2009, pp. 82–85.

13. D. Santano and H. Esmaeili, "Aerial videography in built heritage documentation: The case of post-independence architecture of malaysia," in *International Conference on Virtual Systems & Multimedia*. IEEE, 2014, pp. 323–328.

14. P. Doherty and P. Rudol, "A uav search and rescue scenario with human body detection and geolocalization," in *Australasian Joint Conference on Artificial Intelligence*. Springer, 2007, pp. 1–13.

15. G. Li, X. Zhou, J. Yin, and Q. Xiao, "An uav scheduling and planning method for post-disaster survey," *The International Archives of Photogrammetry, Remote Sensing and Spatial Information Sciences*, vol. 40, no. 2, p. 169, 2014.

16. Q. Wen, H. He, X. Wang, W. Wu, L. Wang, F. Xu, P. Wang, T. Tang, and Y. Lei, "Uav remote sensing hazard assessment in zhouqu debris flow disaster," in *Remote Sensing of the Ocean, Sea Ice, Coastal Waters, and Large Water Regions*, vol. 8175. International Society for Optics and Photonics, 2011, p. 817510.

17. I. Bekmezci, O. K. Sahingoz, and Ş. Temel, "Flying ad-hoc networks (fanets): A survey," *Ad Hoc Networks*, vol. 11, no. 3, pp. 1254–1270, 2013.

18. A. Puri, "A survey of unmanned aerial vehicles (uav) for traffic surveillance," *Technical Report, Department of computer science and engineering, University of South Florida*, pp. 1–29, 2005.

19. A. Chakrabarty and J. Langelaan, "Flight path planning for uav atmospheric energy harvesting using heuristic search," in *AIAA Guidance, Navigation, and Control Conference*, 2010, p. 8033.

20. B. Sumantri, N. Uchiyama, and S. Sano, "Least square based sliding mode control for a quad-rotor helicopter and energy saving by chattering reduction," *Mechanical Systems and Signal Processing*, vol. 66, pp. 769–784, 2016.

21. F. Morbidi, R. Cano, and D. Lara, "Minimum-energy path generation for a quadrotor uav," in *IEEE International Conference on Robotics and Automation (ICRA)*. IEEE, 2016, pp. 1492–1498.

22. X. Lyu, H. Gu, J. Zhou, Z. Li, S. Shen, and F. Zhang, "A hierarchical control approach for a quadrotor tail-sitter vtol uav and experimental verification," in *IEEE International Conference on Intelligent Robots and Systems (IROS)*, 2017.

23. X. Lyu, H. Gu, Y. Wang, Z. Li, S. Shen, and F. Zhang, "Design and implementation of a quadrotor tail-sitter vtol uav," in *IEEE International Conference on Robotics and Automation (ICRA)*, 2017, pp. 3924–3930.

24. H. Gu, X. Cai, J. Zhou, Z. Li, S. Shen, and F. Zhang, "A coordinate descent method for multidisciplinary design optimization of electric-powered winged uavs," *International Conference on Unmanned Aircraft Systems*, pp. 1189–1198, 2018.

25. T. W. Danko, A. Kellas, and P. Y. Oh, "Robotic rotorcraft and perch-and-stare: Sensing landing zones and handling obscurants," in *IEEE International Conference on Advanced Robotics*. IEEE, 2005, pp. 296–302.

26. M. T. Pope, C. W. Kimes, H. Jiang, E. W. Hawkes, M. A. Estrada, C. F. Kerst, W. R. Roderick, A. K. Han, D. L. Christensen, and M. R. Cutkosky, "A multimodal robot for perching and climbing on vertical outdoor surfaces," *IEEE Transactions on Robotics*, vol. 33, no. 1, pp. 38–48, 2017.

27. M. Kovač, J. Germann, C. Hürzeler, R. Y. Siegwart, and D. Floreano, "A perching mechanism for micro aerial vehicles," *Journal of Micro-Nano Mechatronics*, vol. 5, no. 3-4, pp. 77–91, 2009.

28. A. L. Desbiens and M. R. Cutkosky, "Landing and perching on vertical surfaces with microspines for small unmanned air vehicles," *Journal of Intelligent and Robotic Systems*, vol. 57, no. 1-4, p. 313, 2010.

29. A. Lussier Desbiens, A. T. Asbeck, and M. R. Cutkosky, "Landing, perching and taking off from vertical surfaces," *The International Journal of Robotics Research*, vol. 30, no. 3, pp. 355–370, 2011.

30. A. L. Desbiens, A. T. Asbeck, and M. R. Cutkosky, "Scansorial landing and perching," in *Robotics Research*. Springer, 2011, pp. 169–184.

31. D. Mehanovic, J. Bass, T. Courteau, D. Rancourt, and A. L. Desbiens, "Autonomous thrust-assisted perching of a fixed-wing uav on vertical surfaces," in *Conference on Biomimetic and Biohybrid Systems*. Springer, 2017, pp. 302–314.

32. J. Thomas, M. Pope, G. Loianno, E. W. Hawkes, M. A. Estrada, H. Jiang, M. R. Cutkosky, and V. Kumar, "Aggressive flight with quadrotors for perching on inclined surfaces," *Journal of Mechanisms and Robotics*, vol. 8, no. 5, p. 051007, 2016.

33. W. R. Roderick, H. Jiang, S. Wang, D. Lentink, and M. R. Cutkosky, "Bioinspired grippers for natural curved surface perching," in *Conference on Biomimetic and Biohybrid Systems*. Springer, 2017, pp. 604–610.

34. I.-W. Park, T. Smith, H. Sanchez, S. W. Wong, P. Piacenza, and M. Ciocarlie, "Developing a 3-dof compliant perching arm for a free-flying robot on the international space station," in *IEEE International Conference on Advanced Intelligent Mechatronics*. IEEE, 2017, pp. 1135–1141.

35. C. Luo, L. Yu, and P. Ren, "A vision-aided approach to perching a bioinspired unmanned aerial vehicle," *IEEE Transactions on Industrial Electronics*, vol. 65, no. 5, pp. 3976–3984, 2018.

36. M. A. Erbil, S. D. Prior, and A. J. Keane, "Design optimisation of a reconfigurable perching element for vertical take-off and landing unmanned aerial vehicles," *International Journal of Micro Air Vehicles*, vol. 5, no. 3, pp. 207–228, 2013.

37. Z. Zhang, P. Xie, and O. Ma, "Bio-inspired trajectory generation for uav perching," in *IEEE/ASME International Conference on Advanced Intelligent Mechatronics*. IEEE, 2013, pp. 997–1002.

38. ——, "Bio-inspired trajectory generation for uav perching movement based on tau theory," *International Journal of Advanced Robotic Systems*, vol. 11, no. 9, p. 141, 2014.

39. C. E. Doyle, J. J. Bird, T. A. Isom, C. J. Johnson, J. C. Kallman, J. A. Simpson, R. J. King, J. J. Abbott, and M. A. Minor, "Avian-inspired passive perching mechanism for robotic rotorcraft," in *IEEE International Conference on Intelligent Robots and Systems (IROS)*. IEEE, 2011, pp. 4975–4980.

40. C. E. Doyle, J. J. Bird, T. A. Isom, J. C. Kallman, D. F. Bareiss, D. J. Dunlop, R. J. King, J. J. Abbott, and M. A. Minor, "An avian-inspired passive mechanism for quadrotor perching," *IEEE/ASME Transactions on Mechatronics*, vol. 18, no. 2, pp. 506–517, 2013.

41. H. Prahlad, R. Pelrine, S. Stanford, J. Marlow, and R. Kornbluh, "Electroadhesive robots—wall climbing robots enabled by a novel, robust, and electrically controllable adhesion technology," in *IEEE International Conference on Robotics and Automation (ICRA)*. IEEE, 2008, pp. 3028–3033.

42. M. Graule, P. Chirarattananon, S. Fuller, N. Jafferis, K. Ma, M. Spenko, R. Kornbluh, and R. Wood, "Perching and takeoff of a robotic insect on overhangs using switchable electrostatic adhesion," *Science*, vol. 352, no. 6288, pp. 978–982, 2016.

43. H. Jiang, M. T. Pope, E. W. Hawkes, D. L. Christensen, M. A. Estrada, A. Parlier, R. Tran, and M. R. Cutkosky, "Modeling the dynamics of perching with opposed-grip mechanisms," in *IEEE International Conference on Robotics and Automation (ICRA)*. IEEE, 2014, pp. 3102–3108.

44. L. Daler, A. Klaptocz, A. Briod, M. Sitti, and D. Floreano, "A perching mechanism for flying robots using a fibre-based adhesive," in *IEEE International Conference on Robotics and Automation (ICRA)*. IEEE, 2013, pp. 4433–4438.

45. J. Moore and R. Tedrake, "Control synthesis and verification for a perching uav using lqr-trees," in *IEEE Annual Conference on Decision and Control*. IEEE, 2012, pp. 3707–3714.

46. J. Thomas, G. Loianno, M. Pope, E. W. Hawkes, M. A. Estrada, H. Jiang, M. R. Cutkosky, and V. Kumar, "Planning and control of aggressive maneuvers for perching on inclined and vertical surfaces," in *ASME International Design Engineering Technical Conferences and Computers and Information in Engineering Conference*. American Society of Mechanical Engineers, 2015.

47. R. Cory and R. Tedrake, "Experiments in fixed-wing uav perching," in *AIAA Guidance, Navigation and Control Conference and Exhibit*, 2008, p. 7256.

48. K. Zhang, P. Chermprayong, T. Alhinai, R. Siddall, and M. Kovac, "Spidermav: Perching and stabilizing micro aerial vehicles with bio-inspired tensile anchoring systems," in *IEEE International Conference on Intelligent Robots and Systems (IROS)*. IEEE, 2017, pp. 6849–6854.

49. Q. Delamare, P. R. Giordano, and A. Franchi, "Toward aerial physical locomotion: The contact-fly-contact problem," *IEEE Robotics and Automation Letters*, vol. 3, no. 3, pp. 1514–1521, 2018.

50. A. M. Berg and A. A. Biewener, "Wing and body kinematics of takeoff and landing flight in the pigeon (columba livia)," *Journal of Experimental Biology*, vol. 213, no. 10, pp. 1651–1658, 2010.

51. H. Song, M. Y. Wang, and K. Hang, "Fingertip surface optimization for robust grasping on contact primitives," *IEEE Robotics and Automation Letters*, vol. 3, no. 2, pp. 742–749, 2018.

52. D. Mellinger, N. Michael, and V. Kumar, "Trajectory generation and control for precise aggressive maneuvers with quadrotors," *The International Journal of Robotics Research*, vol. 31, no. 5, pp. 664–674, 2012.

53. D. Mellinger, M. Shomin, N. Michael, and V. Kumar, "Cooperative grasping and transport using multiple quadrotors," in *Distributed autonomous robotic systems*. Springer, 2013, pp. 545–558.

54. S.-J. Kim, D.-Y. Lee, G.-P. Jung, and K.-J. Cho, "An origami-inspired, self-locking robotic arm that can be folded flat," *Science Robotics*, vol. 3, no. 16, p. eaar2915, 2018.

55. P. E. I. Pounds, D. R. Bersak, and A. M. Dollar, "Grasping from the air: Hovering capture and load stability," in *IEEE International Conference on Robotics and Automation (ICRA)*, May 2011, pp. 2491–2498.

56. R. B. Rusu and S. Cousins, "3D is here: Point Cloud Library (PCL)," in *IEEE International Conference on Robotics and Automation (ICRA)*, Shanghai, China, May 9-13 2011.

57. D. Mellinger and V. Kumar, "Minimum snap trajectory generation and control for quadrotors," in *IEEE International Conference on Robotics and Automation (ICRA)*. IEEE, 2011, pp. 2520–2525.

58. J. Solà, "Quaternion kinematics for the error-state kalman filter," *CoRR*, vol. abs/1711.02508, 2017.

5 Acknowledgments

Funding: This work was supported by Knut and Alice Wallenberg Foundation, Swedish Research Council, HKUST Initiation grant 16EG09, and Hong Kong Innovation Technology Fund (ITS/334/15FP). **Author contributions**: K.H. proposed the design principals, designed the modular landing gear, implemented the vision detector, analyzed data, and wrote part of the manuscript; X.L. designed part of the landing gear and performed all the experiments; H.S. Designed contact modules and fabricated the landing gear; J.A.S. advised for the design principals and the experiment design, formulated the scientific questions, analyzed data, and wrote part of the paper; A.M.D. advised and supervised the project; D.K. provided funding and supervised the project; F.Z. provided funding and supervised the project. **Data and materials availability**: All data needed to evaluate the conclusions in the paper are present in the paper or the Supplementary Materials. Additional information can be addressed to K.H..

6 Supplementary materials

Appendix S1. Flight Controller Design.

Table S1. Weights of Parts.

Movie S1. Perching and resting actions test.

Reference(58)

Flight Controller Design

Supplementary Document

The controller structure of our vehicle is detailed in Fig. 1, which consists of a position controller (shown in Fig. 2), an attitude controller (shown in Fig. 3), and a mixer.

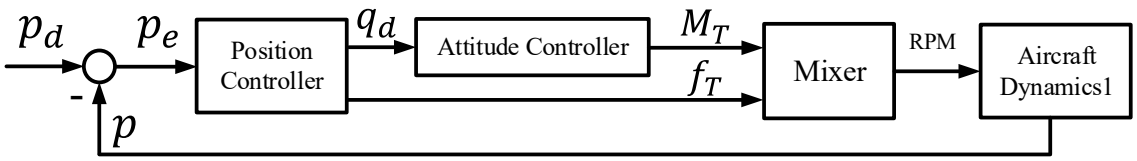

Fig. 1: Controller structure

The position controller is a cascaded controller, including a position loop which is a proportional controller and a velocity loop which is a PID controller. Through the *Thrust & Attitude Calculator* module, the inertial force vector f_i is transformed to the vehicle thrust f_T and the desired attitude R_d in $SO(3)$ (57). The vehicle thrust can be calculated by

$$\begin{aligned} p_e &= p_d - p \\ v_d &= k_p p_e \\ v_e &= v_d - v \\ f_i &= K_p v_e + K_i \int v_e dt + K_d \frac{dv_e}{dt} + \begin{bmatrix} 0 & 0 & -mg \end{bmatrix}^T \\ f_T &= f_i \cdot z_b \end{aligned} \tag{1}$$

where p_d, p, and p_e are respectively the designed position, the estimated position and the position error. v_d, v, and v_e are respectively the designed velocity, the estimated velocity and the velocity error. k_p is a positive diagonal gain for the proportional controller. K_p, K_i, and K_d are positive diagonal gains for the PID controller. The desired

attitude is computed as

$$
\begin{aligned}
z_b^d &= \frac{f_i}{\|f_i\|} \\
x_c^d &= \begin{bmatrix} \cos(\psi_d) & \sin(\psi_d) & 0 \end{bmatrix}^T \\
y_b^d &= \frac{z_b^d \times x_c^d}{\|z_b^d \times x_c^d\|} \\
x_b^d &= y_b^d \times z_b^d \\
R_d &= \begin{bmatrix} x_b^d & y_b^d & z_b^d \end{bmatrix}
\end{aligned}
\tag{2}
$$

where x_b^d, y_b^d, and z_b^d are the desired body axis vectors represented in the inertial frame, y_c^d is the desired intermediate axis vector represented in the inertial frame.

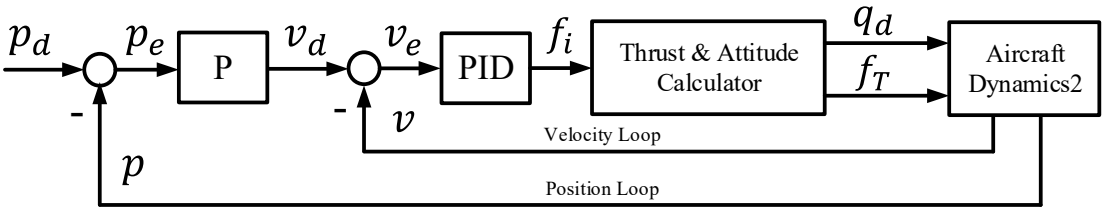

Fig. 2: Position controller

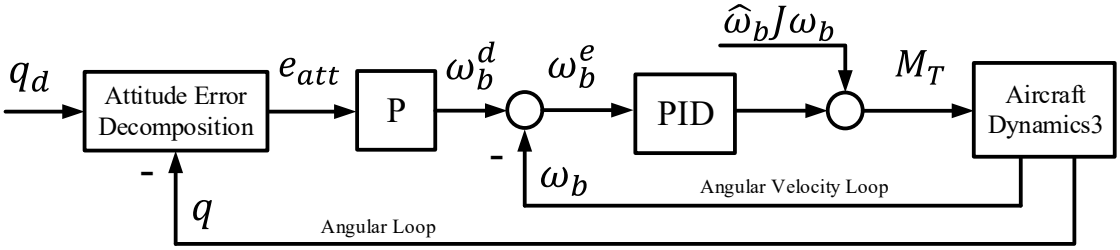

Fig. 3: Attitude controller

Thereafter, the desired attitude R_d is converted to q_d and fed to the cascaded attitude controller as shown in Fig. 3. The *Linear Quaternion* method presented in (22, 23) is used to calculate the attitude error e_{att}, which can

be written as

$$
\begin{aligned}
q_e &= {q_d}^* \otimes q = \begin{bmatrix} q_{e0} & q_{e1} & q_{e2} & q_{e3} \end{bmatrix}^T = \begin{bmatrix} \eta_e & \epsilon_e^T \end{bmatrix}^T \\
\varphi &= \begin{cases} 2\sin^{-1}\left(\|\epsilon_e\|\right); & \|\epsilon_e\| \leq \dfrac{\sqrt{2}}{2} \\ 2\cos^{-1}\left(|\eta_e|\right); & \dfrac{\sqrt{2}}{2} < \|\epsilon_e\| \leq 1 \end{cases} \\
e_{att} &= \frac{\varphi}{\sin\frac{\varphi}{2}} \cdot \epsilon_e
\end{aligned}
\tag{3}
$$

where q_d, q, and q_e are respectively the reference attitude, the actual attitude, and the attitude error represented in quaternion. The first entry of the quaternion is a scalar and the remaining three parameters are vectors. η_e and ϵ_e are the scalar and the vector part of the attitude error quaternion, respectively. $(\cdot)^*$ is the conjugate of a quaternion, and $\otimes$ is the quaternion product (58). φ is the rotation angle. Once the attitude error vector is obtained, the reference angular velocity in the body frame can be written as

$$
w_b^d = -k_p e_{att}, k_p > 0 \tag{4}
$$

The inner loop is a PID controller, for which a feed-forward term is added to cancel the Coriolis term. The control algorithm can be written as

$$
M_T = K_p w_b^e + K_i \int w_b^e dt + K_d \frac{dw_b^e}{dt} + \hat{w}_b J w_b \tag{5}
$$

where $M_T = \begin{bmatrix} M_{Tx} & M_{Ty} & M_{Tz} \end{bmatrix}^T \in \mathbb{R}^3$ is the moment vector, K_p, K_i, and K_d are positive diagonal gains for the PID controller, $w_b^e = w_b^d - w_b$ is the angular velocity error. Using this method, the attitude can be well decoupled and controlled independently in roll, pitch, and yaw directions.

Once the M_T and f_T are obtained, a mixer is used to allocate the rotation speed of each rotor, which can be written as

$$
\begin{aligned}
\begin{bmatrix} T_1 \\ T_2 \\ T_3 \\ T_4 \end{bmatrix} &= \begin{bmatrix} 1 & -1 & 1 & -1 \\ 1 & 1 & 1 & 1 \\ 1 & -1 & -1 & 1 \\ 1 & 1 & -1 & -1 \end{bmatrix} \begin{bmatrix} f_{Tz} \\ \frac{\sqrt{2}M_{Tx}}{d} \\ \frac{\sqrt{2}M_{Ty}}{d} \\ \frac{M_{Tz}}{\kappa} \end{bmatrix} \\
\kappa &= \frac{c_q}{c_t} \\
\varpi_i &= \sqrt{\frac{T_i}{c_t}} \quad (i = 1, 2, 3, 4)
\end{aligned}
\tag{6}
$$

where d is the arm length of each motor. T_i and $\varpi_i (i = 1, 2, 3, 4)$ are respectively the rotor thrust and rotation speed (in RPM), c_q is propeller torque coefficient, c_t is propeller thrust coefficient, and κ is the ratio between the torque and trust coefficients.

Table S1: Weights of Parts

Part	Material	Weight (g)
DJI F450	–	760
Landing Gear Base	Carbon Fiber	115
Leg	Carbon Fiber	25
Battery	–	360
Servo Motor	–	60
EEF 1	TangoBlackPlus	66
EEF 2	TangoBlackPlus	39
EEF 3	PC ABS	13